

PREOXIDATION EFFECTS ON THE ENERGETICS OF RAPID COAL PYROLYSIS

Hyok. B. Kwon
Department of Environmental Engineering
Kyungnam University, 449 Wolyoungdong Masan, 631-701 KOREA
and
Francis J. Vastola
Department of Materials Science and Engineering
Pennsylvania State University, University Park, PA 16802, U.S.A.

Keywords: rapid coal pyrolysis, preoxidation, energetics

INTRODUCTION

Thermophysical properties such as the pyroheat, specific pyroheat, and heat of pyrolysis of coal are important energetic data in design computations relating to various coal utilization processes. Moreover, these properties of coal continuously change during pyrolysis. Therefore, knowledge of the thermophysical properties of coal under conditions of rapid heating over a wide dynamic temperature range has important implications with respect to practical usage and fundamental research of coal. The endothermic heat effects during rapid coal pyrolysis have been identified qualitatively (1, 2) and quantitatively (3-5). Of particular interest in this work is the examination of the preoxidation effects on the energetics of rapid coal pyrolysis. This interest arises from the fact that mild preoxidation inevitably occurs during handling and storage prior to practical usage. This phenomenon is known as weathering and can alter the coal's calorific value, thermoplastic properties, beneficiation, coking, liquefaction, and gasification characteristics. This mild preoxidation also influence standard tests and other experimental results, and thus has important implications with respect to fundamental research on the structure and properties of coal. The objectives of this study were to determine the preoxidation effects upon subsequent pyrolysis energetics of a subbituminous coal.

EXPERIMENTAL

Apparatus. The main components of the calorimeter are the grid reactor, electrical system, and microcomputer. The microcomputer is coupled with the reactor through a voltage regulator and a multiplexed analog/digital converter for process control and data acquisition. Details of the apparatus and procedure are given elsewhere (3). The reactor is a SS (Type 315) grid which is electrically heated by a constant voltage power supply. Heating rates were controlled by an adjustable voltage regulator powered by an acid-lead battery. The low internal resistance batteries and regulator insure constant voltage at high currents (Figure 1). The SS mesh grid and a brass bar, used as a reference resistance, make up the heating circuit. The low resistance (5.17m Ω) and large mass (50g) of the reference resistor minimize the changes in resistance from the variation in temperature due to resistive heating. Therefore, the reference resistance can be assumed to be constant during the experiment. The pyrolysis temperature, defined as the temperature at the middle of the grid, is determined from a thin (50 μ m) chromel-alumel thermocouple. For a given constant voltage the grid temperature reaches a steady state at which the resistive heat input balances losses by heat transfer. After being held at the final steady state temperature for the desired time, the sample is cooled by turning the power off.

Calibration. A number of substances (Sn, Zn, Al; Aldrich Chemical Co., 5N) undergoing phase transitions at temperatures up to 933 K were tested (Table 1). Temperature calibration was carried out with melting temperatures of standard substances. At the same time, calorimetric calibration was carried out by using the enthalpies of fusion of substances at their temperatures.

Sample Selection. Coal samples were obtained from the Penn State coal sample bank. Proximate and ultimate analyses of the coals are provided by the Penn State coal database and are presented in Table 2.

Experimental Conditions. Experimental conditions are listed below:

1. sample size ; 6.5 \pm 1.0 mg
2. particle size ; 100 microns (140 x 170 mesh)
3. drying ; vacuum dry overnight at 383 K
and in situ for 10 min. at 393 K
4. duration of reaction ; 20 sec
5. final temperature ; 920 \pm 20 K
6. heating rate ; 415 \pm 30 K/s at 0.2 sec
7. soaking time ; 15 sec
8. data acquisition interval ; 20 ms
9. preoxidation level ; 1, 5, 10 and 24 hrs at 400 K
with air in horizontal furnace

Procedure. After a thermocouple was welded to a new mesh, which was folded into a "sandwich" heating element, forming a 2.5 x 12 mm strip and connected across the electrodes, the cell was evacuated, charged with nitrogen gas, and pre-fired to prevent further physical and chemical change of the mesh. During the pre-firing, the mesh expanded and annealed until it reached a steady state condition. Then, 5-10 mg of coal sample was loaded into the mesh. The particles had a uniform diameter of approximately 100 μm (140 x 170 US mesh). After the coal was loaded, the cell was charged with nitrogen gas. The coal was dried inside the reactor for 10 minutes at 393 K. Next, the coal-grid system was heated with a constant voltage pulse, then cooled via simple heat dissipation. The remaining grid-char runs were made.

Data Reduction. In order to derive the thermal properties from the raw data, it is necessary to follow the reduction procedure which is described below and graphed in Figure 2. The interpretation of each symbol is given in Table 3. Figure 1 shows the equivalent electrical circuit of the reactor. By measuring at 20 ms intervals, the two voltages e_s , e_r , and $e_{s,r}$, the temperature of the system can be measured and the power input to the system, W_i , can be calculated versus time.

$$W_i = \frac{e_s e_r}{R_r}$$

The power loss from the system at a given temperature can be calculated by determining the convective and radiative heat loss versus temperature according to the expression

$$W_l = A(T_g - T_m) + B(T_g^4 - T_m^4)$$

The terms A and B can be obtained experimentally at the end of a char run by heating the system to a series of temperature and fitting the data to above equation using an iterative technique. A check can be made to ascertain whether the radiation coefficient, B, is physically valid or not by comparing emissivity. By being able to measure the power input to the system versus time and temperature and by being able to calculate the power loss from the system versus temperature, net power absorbed by the system versus time can be calculated. From these values the integral of heat absorbed by the system versus time can be obtained. Each run would consist of three heatings, the grid alone, the coal sample in the grid, and finally the char remaining in the grid. By being able to normalize the runs to power absorbed versus temperature, the net heat absorbed by the grid, coal, and char is obtained (Figure 2d). The subtraction of the heat absorbed by the grid from that of the coal and the char runs enables the net heat requirements for heating the coal and the char to the final temperature to be obtained. The heat of pyrolysis is arrived at by subtracting the net heat absorbed by the char from that of the coal (Figure 2e). The differential of these values is shown in Figure 2f.

Preoxidation of Coal Sample. Preoxidized coal samples were prepared corresponding with 1, 5, 10, and 24 hrs of air exposure at 400 K with a horizontal furnace. Coal samples were dried 1 hr at 400 K, with nitrogen purging before oxidation. Oxygen uptake on coal samples was monitored as the gain in weight by a Fisher TGA system. Approximately 10 mg of coal were placed in the platinum sample bucket and the system was flushed with nitrogen (flow rate of 100 cc/min) for 20 min to displace air. The sample was then heated to 400 K and held at that temperature for 1 hr for drying. The nitrogen flow was then switched to dry air and changes in sample weight were monitored in time. The results are presented in Figure 3. As illustrated, the coal samples used in this study show a very mild oxygen chemisorption of 0.7% oxygen uptake after 10 hrs of air exposure. Since there is the strong possibility that gasification takes place even at the preoxidation temperature used in this study, values obtained from this thermogravimetric method provide a lower limit for the amount of oxygen added rather than an absolute one.

Estimation of Volatile Yields. Due to the reactor design, the weighing of the resulting char was difficult; therefore, the mass of remaining char could not be measured directly. Rather, the mass was estimated using heat capacity as an indicator. The basic assumption applied is that the heat capacity of char produced from the slow heating is equal to the heat capacity of char produced from rapid heating. That is, it is assumed that the heating rate will not affect the heat capacity of the remaining char. Then the mass of the char resulting from the coal pyrolysis was calculated from the experimental heat capacity data and the volatile yield was estimated. To assess the errors associated with assumption, the heat capacity of the char produced from rapid heating was also determined on a known mass basis.

RESULTS AND DISCUSSION

The thermophysical properties measured were 1) pyroheat, ΔH_{ph} , which is the energy required to heat coal to a given temperature and is the sum of the heat of pyrolysis and heat capacity over the heating temperature interval; 2) pyroheat capacity, C_{ph} , which is the pyroheat normalized over a differential temperature interval; 3) heat of pyrolysis, ΔH_{py} , which is the thermal difference between heating coal and char to the same final temperature; and 4) pyrolysis heat capacity, C_{py} , which is the heat of pyrolysis normalized over a differential temperature interval. The experimental results are presented in Tables 4 through 6.

Pyroheat. As can be seen from Table 4, pyroheat increases as temperature increases in the temperature range from room temperature to 900 K. And the unoxidized coal was the most endothermic and that the coal with the highest degree of preoxidation was the least endothermic during the pyrolysis. The pyroheats of unoxidized PSOC 64B, subbituminous B coal and the coal exposed at 400 K for 24 hrs are 993 J/g and 756 J/g at 900 K, respectively.

Pyroheat Capacity. The pyroheat capacity of coal increases up to 650 K as the energy demanded for the pyrolyzing coal increases. Above 650 K, the endothermic effect decreases and the pyroheat capacity falls to the same value as the char (Table 5). The pyroheat capacity of the char at 900 K decreases from 1.29 J/gK to 0.98 J/gK as the level of preoxidation increases. The maximum pyroheat capacities of unoxidized coal and the coal exposed at 400 K for 24 hrs are 2.16 J/gK at 610 K and 1.62 J/gK at 640 K, respectively.

Heat of Pyrolysis. The effects of preoxidation on the apparent heat of pyrolysis are presented in Figure 4. It shows that a 20% reduction in apparent heat of pyrolysis occurs within the first 10 hrs for the preoxidized coal sample. After this time interval, the apparent heat of pyrolysis approaches asymptotic values of 25% reduction. However, the effects of preoxidation could be appreciated more realistically if one examines the effective heat of pyrolysis, which is based on the actual participating fraction. Table 8 shows that the drastic 17% reduction for the coal preoxidized for 1 hrs continuously decreased to a 58% reduction for the coal preoxidized for 24 hrs. At the mild levels of preoxidation employed in this study, the effects on energetics were drastic. For example, the thermogravimetric results show that mild preoxidation of PSOC 64B resulted in only a slight oxygen uptake. However, under the rapid heating conditions, effective heat of pyrolysis for mildly preoxidized samples are reduced 58% when compared with the corresponding effective heat of pyrolysis for the unoxidized coals. The apparent heat of pyrolysis of unoxidized coal and the coal preoxidized for 24 hrs are 316 J/g and 242 J/g, respectively. The effective heat of pyrolysis of unoxidized coal and the coal preoxidized for 24 hrs are 1086 J/g and 456 J/g, respectively (Figure 5). For the preoxidized coals, the temperature at which maximum pyrolysis occurs shifts to higher temperature. However, after the initial oxidation, the temperature at which maximum pyrolysis occurs is not changed with further oxidation.

Effects of Preoxidation. The preoxidation effects on subsequent pyrolysis behavior are summarized in Table 8. The heats of pyrolysis decrease with the level of preoxidation. However, volatile yields increase with the level of preoxidation. The estimated mass of the char decreases from 70.9% to 46.9% of its original sample mass with the level of preoxidation. In other words, volatile yields increase from 29.1% to 53.1% with the level of preoxidation. Volatile yields increase from 22.5% to 29.1% as the heating rate increase from 2 K/s to 400 K/s. The heating rate effect is enhanced with preoxidation. For example, volatile yields increase with preoxidation from 22.5% to 35.4% for a 2 K/s heating rate, while volatile yields increase from 29.1% to 53.1% for a 400 K/s heating rate (Table 9). Rapid heating generates higher pressure inside of coal very quickly due to increased rate of pyrolysis. The increased pressure differential enables the pyrolysis products to more rapidly leave the coal mass with much less chance of cracking and secondary reaction. Consequently, rapid heating increases the carbon removal efficiency of hydrogen, which results in the increased volatile yields of pyrolysis. Furthermore, preoxidation results in an activating effect on the bond breaking reaction. Therefore, the heating rate effect is enhanced by the preoxidation. The preoxidation effects on the volatile yields of pyrolysis are presented in Figure 6. The effect of preoxidation on both energetics and volatile yields of pyrolysis could be attributed to the oxygen functional groups, especially the phenolic-OH group. The phenolic-OH groups could reduce the endothermicity of the fragmentation reaction by their activating effect on bond breaking. The volatile yields increase with the heating rate. This heating rate effect is enhanced by the preoxidation due to its reducing effect on endothermicity, which results in the efficient use of a given energy. In summary, rapid heating causes more extensive fragmentation of preoxidized coal when compared with unoxidized coal. This demonstrates that the preoxidation causes a change in molecular structure and leads to the extensive fragmentation of preoxidized coal.

CONCLUSIONS

The effect of preoxidation on the subsequent rapid pyrolysis behavior is significant. Mild preoxidation reduces the endothermicity of pyrolysis drastically. The unoxidized coal is the most endothermic and the coal with the highest degree of preoxidation is the least endothermic during the pyrolysis. As a result, pyroheat, pyroheat capacity, and heat of pyrolysis decrease as the degree of preoxidation increases. The volatile yields increase with the level of preoxidation. The apparent heat of pyrolysis of unoxidized coal and coal preoxidized at 400 K with air for 24 hrs are 316 J/g and 242 J/g at 900 K, respectively. Their maximum pyroheat capacities are 0.96 J/gK at 590 K and 0.7 J/gK at 630K, respectively. The effective heat of pyrolysis of unoxidized coal and the coal preoxidized for 24 hrs are 1086 J/g and 456 J/g, respectively. The yields of volatiles for unoxidized

and preoxidized coal are 29.1% and 53.1%, respectively. However, the yields of volatiles with complementary slow heating (2 K/s) for unoxidized coal and preoxidized coal are 22.5% and 35.4%, respectively.

ACKNOWLEDGEMENTS

This study was made possible by financial support from the Coal Cooperative Program at The Pennsylvania State University. The authors thank the Penn State Coal Sample Bank and Data Base for supplying the sample and the analysis of the coal used in this study.

REFERENCES

1. Freihaut, J.D.; Zabielski, M.F.; Serry, D.J. *Prepr. Am. Chem. Soc., Div. Fuel Chem.* **1982**, *27*, 89-98.
2. Morel, O.; Vastola, F.J. *Prepr. Am. Chem. Soc., Div. Fuel Chem.* **1984**, *29*, 77-82.
3. Kwon, H.B., Ph.D. Thesis, Pennsylvania State University, **1987**.
4. Kwon, H.B.; Vastola, F.J. *Prepr. Am. Chem. Soc., Div. Fuel Chem.* **1993**, *38(4)*, 1168-1177.
5. Kwon, H.B.; Vastola, F.J. *Fuel Process. Technol.* **1995**, *44*, 13-24.

Table 1. Calibration

Standard substance	Literature		Measured	
	m.p.(K)	ΔH fusion(J/g)	m.p.(K)	ΔH fusion(J/g)
Sn	505.1	60.7	496	71
			496	67
			495	70
Zn	692.7	113.0	688	120
			690	127
			691	125
Al	933.5	396.0	928	414
			920	423
			932	450

Table 2. Characteristics of coal used

PSU/DOE Ident. Number: PSOC-64B

Apparent Rank : Sub-bituminous B

Seam: Monarch , Wyoming

Mine: Big Horn

Proximate Analysis, wt. %:	As Rec'd	dry	daf
Moisture	22.1	-	-
Ash	4.6	5.9	-
Volatile Matter	33.7	43.3	46.0
Fixed Carbon	39.6	50.8	54.0
Ultimate Analysis, Wt. %:	As Rec'd*	dry	daf
C	53.0	68.1	72.3
H	4.0	5.1	5.5
N	0.8	1.0	1.1
S(total)	0.3	0.4	0.5
O(by difference)	15.2	19.5	20.7

*Excludes Moisture

Calorific value, kJ/g:

dmmc	28.1
dmmf	28.9

Table 3. Data reduction symbols

English symbols

A	Coefficient for conduction and convection
B	Coefficient for radiation
e	Voltage drop
H	Enthalpy
I	Current
R	Resistance
T	Temperature
W	Power

Subscripts

g	Grid
i	Input
l	Loss
r	Reference
s	System
rm	Room
tc	Thermocouple

Table 4. Pyroheat and Specific Pyroheat of Coal

Preoxidation Time(hr)	0		1		5		10		24	
Temperature (K)	ΔH_{ph} (J/g)	C _{ph} (J/gK)								
350	47	0.73	50	0.65	40	0.65	36	0.56	37	0.55
375	71	0.93	73	0.85	62	0.81	56	0.72	57	0.71
400	99	1.14	102	1.04	89	0.97	80	0.87	78	0.86
425	132	1.33	131	1.23	118	1.11	106	1.02	104	0.99
450	171	1.52	167	1.42	148	1.25	135	1.17	133	1.11
475	213	1.70	207	1.60	182	1.39	167	1.30	166	1.23
500	260	1.85	252	1.77	219	1.51	201	1.42	199	1.33
525	311	1.98	302	1.91	261	1.62	243	1.52	232	1.42
550	365	2.07	357	2.01	306	1.71	286	1.59	273	1.50
575	428	2.13	414	2.09	352	1.78	330	1.64	317	1.55
600	483	2.16	467	2.14	401	1.81	372	1.67	355	1.60
625	533	2.16	53	2.16	450	1.81	415	1.69	396	1.62
650	594	2.13	580	2.17	499	1.79	459	1.68	439	1.62
675	648	2.06	631	2.13	543	1.73	502	1.64	480	1.58
700	699	1.95	690	2.03	585	1.63	546	1.57	522	1.50
725	749	1.81	743	1.87	629	1.50	585	1.47	564	1.39
750	797	1.68	791	1.67	669	1.36	623	1.36	598	1.27
775	835	1.55	830	1.49	698	1.21	652	1.26	623	1.15
800	862	1.44	859	1.38	724	1.11	679	1.17	646	1.07
825	894	1.36	876	1.31	744	1.05	701	1.12	667	1.02
850	926	1.32	901	1.27	765	1.02	729	1.09	689	0.99
875	959	1.30	934	1.25	796	1.01	761	1.08	723	0.98
900	993	1.29	967	1.25	827	1.01	793	1.07	756	0.97

Table 5. Pyroheat and Specific Pyroheat of Char

Preoxidation Time(hr)	0		1		5		10		24	
Temperature (K)	ΔH_{ph} (J/g)	C _{ph} (J/gK)								
350	35	0.49	38	0.48	30	0.41	28	0.38	30	0.37
375	53	0.60	56	0.60	44	0.51	42	0.47	43	0.46
400	71	0.70	76	0.70	60	0.61	58	0.55	58	0.54
425	92	0.79	95	0.79	79	0.68	74	0.63	74	0.61
450	113	0.88	119	0.86	100	0.75	91	0.70	92	0.67
475	136	0.95	143	0.93	120	0.79	110	0.77	109	0.72
500	164	1.02	167	0.98	142	0.82	130	0.82	129	0.76
525	192	1.07	194	1.03	165	0.84	155	0.86	150	0.80
550	217	1.12	222	1.07	188	0.86	178	0.90	171	0.84
575	250	1.16	250	1.11	209	0.87	201	0.93	192	0.87
600	280	1.20	277	1.15	229	0.89	224	0.95	215	0.90
625	312	1.25	306	1.19	252	0.90	250	0.97	239	0.91
650	340	1.30	339	1.22	274	0.92	275	0.99	264	0.93
675	375	1.33	371	1.23	298	0.94	300	1.00	287	0.94
700	409	1.34	404	1.25	323	0.95	325	1.01	309	0.96
725	445	1.34	435	1.26	348	0.96	350	1.03	333	0.98
750	484	1.34	465	1.28	370	0.98	378	1.05	359	1.00
775	513	1.33	497	1.29	395	0.98	404	1.06	358	1.01
800	548	1.32	531	1.27	419	0.99	429	1.06	409	1.01
825	577	1.31	564	1.25	446	0.98	457	1.05	436	1.00
850	614	1.30	600	1.23	472	0.98	487	1.04	464	0.99
875	645	1.29	629	1.21	498	0.97	516	1.03	491	0.98
900	677	1.29	661	1.21	524	0.97	541	1.03	514	0.98

Table 6. Pyroheat and Specific Pyroheat of Pyrolysis

Preoxidation Time(hr)	0		1		5		10		24	
	ΔH_{ph} (J/g)	C _{ph} (J/gK)								
350	11	0.21	11	0.13	9	0.21	8	0.15	7	0.15
375	17	0.30	16	0.20	17	0.27	13	0.21	14	0.21
400	27	0.40	25	0.28	28	0.33	21	0.28	19	0.27
425	40	0.50	34	0.37	38	0.40	32	0.35	28	0.34
450	57	0.61	46	0.48	47	0.48	43	0.42	40	0.41
475	76	0.71	63	0.59	61	0.56	56	0.49	55	0.47
500	95	0.80	84	0.71	76	0.65	70	0.56	68	0.54
525	118	0.88	107	0.81	95	0.75	87	0.62	81	0.59
550	147	0.93	133	0.89	118	0.82	107	0.66	102	0.63
575	177	0.96	163	0.94	142	0.88	128	0.69	124	0.66
600	202	0.96	189	0.97	170	0.91	147	0.71	139	0.69
625	220	0.92	216	0.97	197	0.91	164	0.71	155	0.70
650	253	0.86	240	0.96	224	0.88	182	0.70	175	0.70
675	273	0.77	258	0.93	245	0.82	201	0.66	192	0.66
700	290	0.65	286	0.85	262	0.72	220	0.59	212	0.58
725	303	0.52	307	0.72	281	0.59	234	0.50	230	0.48
750	312	0.39	325	0.53	298	0.44	245	0.38	239	0.35
775	322	0.27	333	0.35	302	0.29	248	0.27	237	0.22
800	313	0.16	327	0.20	304	0.17	248	0.17	236	0.12
825	316	0.08	311	0.12	297	0.09	243	0.11	230	0.05
850	312	0.03	300	0.07	291	0.05	241	0.07	224	0.02
875	313	0.01	304	0.05	298	0.04	244	0.05	231	0.00
900	316	0.00	306	0.00	303	0.00	252	0.00	242	0.00

Table 7. Estimation of Volatile Yields

Heating Rate of Coal Run (k/s)	Volatile Yields(%)					
	Preoxidation Time (hrs) *					
	0	1	5	10	24	
C _p , char (J/gk), orig. mass of coal	400	1.29	1.21	0.97	1.03	0.98
C _p , char (J/gk), known mass of char	0.2	1.82	1.83	1.9	1.94	2.09
	400	1.84				
Mass of Char (%) at 900 K, estimated	400	70.9	66.1	51.1	53.1	46.9
Volatile Yields (%), estimated	400	29.1	33.9	48.9	46.9	53.1

* At 400 K with air

Table 8. Effects of Preoxidation on Subsequent Pyrolysis Behavior (At 900 K with a 400 k/s Heating Rate)

	Preoxidation Time (hrs) *				
	0	1	5	10	24
Variation in Ap. Heat of Pyrolysis	1	0.97	0.96	0.8	0.77
Variation in Ef. Heat of Pyrolysis	1	0.83	0.57	0.49	0.42
Variation in Volatile Yields	1	1.16	1.68	1.61	1.82
Volatile Yields (%)	29.1	33.9	48.9	46.9	53.1
Apparent Heat of Pyrolysis (J/g)	316	306	303	252	242
pyroheat of Char (J/g)	677	661	524	541	514
Pyroheat of Coal (J/g)	993	967	827	793	756
Effective Heat of Pyrolysis (J/g)	1086	903	620	537	456

* At 400 K with air

Table 9. Effects of Heating Rate on Volatile Yields

Heating Rate of Coal Run (k/s)	Volatile Yields (%)				
	preoxidation Time (hrs) *				
	0	1	5	10	24
0.2	36.5	36.8	36.1	35.9	35.9
2	22.5			26.8	35.4
400	29.1	33.9	48.9	46.9	53.1

* At 400 K with air

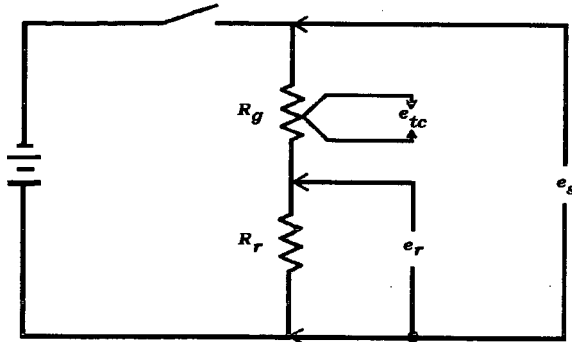


Fig. 1. Equivalent circuit of the heating system

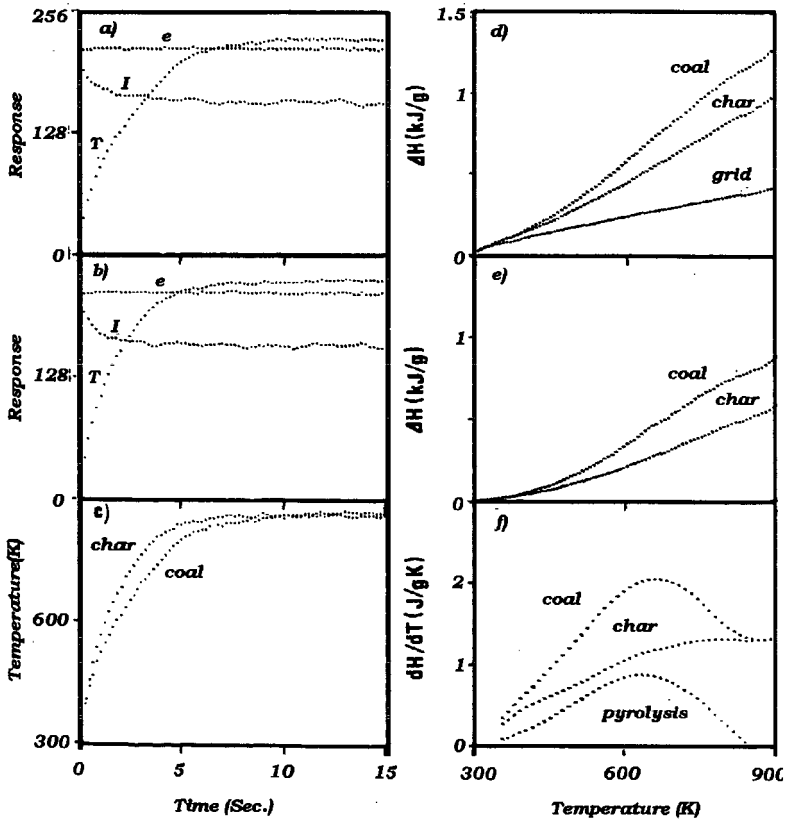


Fig 2. Data reduction: Coal run (a), char run (b), temperature profile (c), enthalpy change (d), normalized enthalpy change (e), and rate of enthalpy change (f).

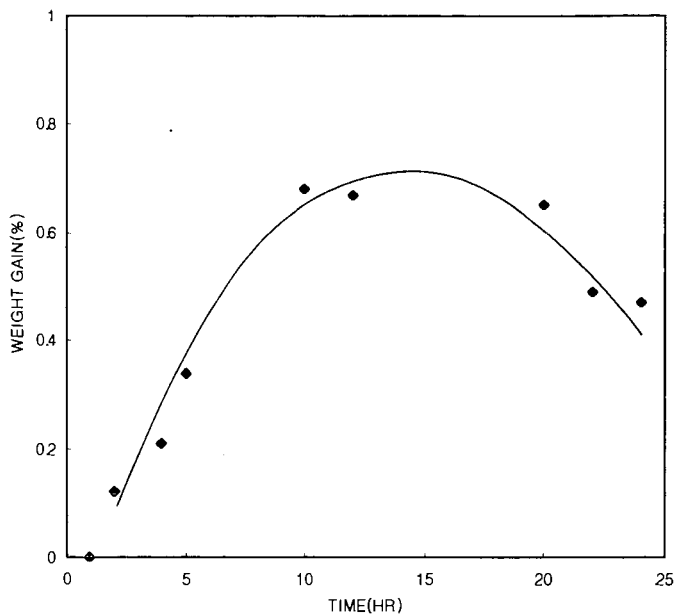


Fig 3. Weight Gain vs. Preoxidation Time

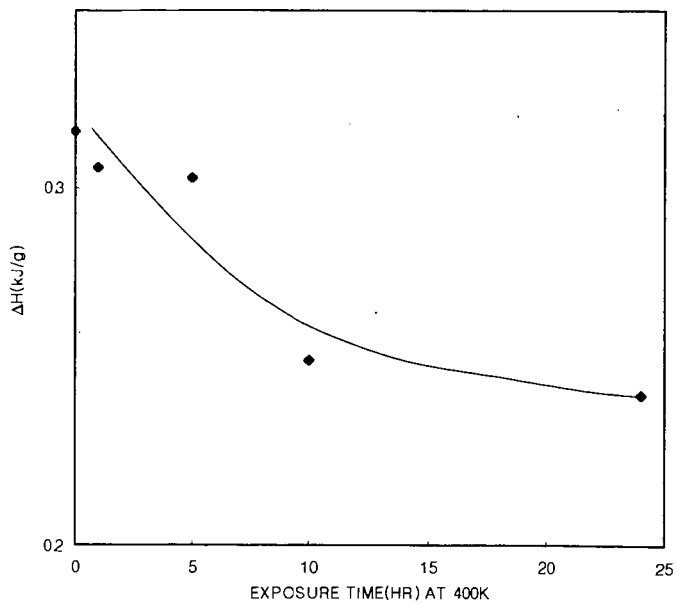


Figure 4. Apparent Heat of Pyrolysis (at 900 K) vs. Preoxidation Time

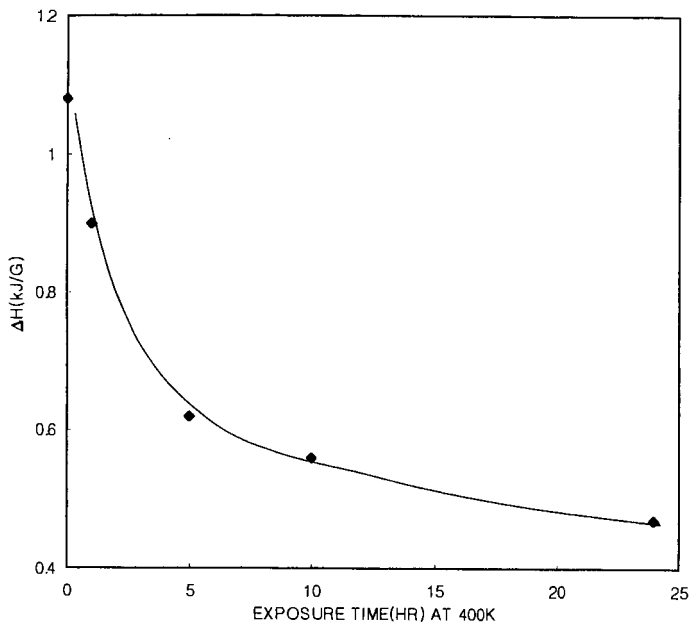


Figure 5. Effective Heat of Pyrolysis (at 900 K) vs. Preoxidation Time

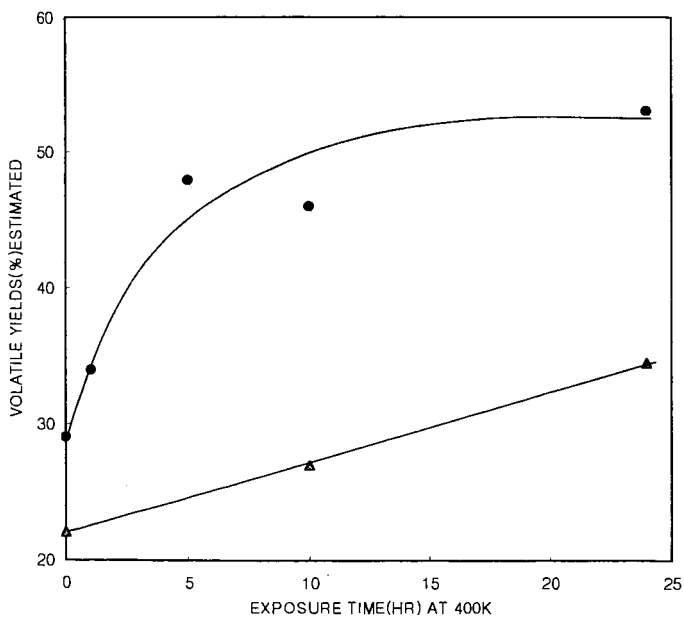


Figure 6. Volatile yields of pyrolysis (at 900 K) vs. Preoxidation Time for Different Heating Rates Heating Rate (K/s); 2(▲) and 400(●)